Template Matching for Detection of Starry Milia-Like Cysts in Dermoscopic Images

Viswanaath Subramanian[1], Randy H. Moss[1], Ryan K. Rader[2],
Sneha K. Mahajan[1] and William V. Stoecker[1,2]
[1]*Department of Electrical and Computer Engineering, Missouri University of Science & Technology, 141 Emerson Electric Co. Hall, Rolla, MO, U.S.A.*
[2]*Stoecker & Associates, 10101 Stoltz Drive, Rolla, MO, U.S.A.*

Keywords: Pattern Analysis, Image Processing, Object Detection, Template Matching, Seborrheic Keratosis, Milia-Like Cysts.

Abstract: Early detection of melanoma by magnified visible-light imaging (dermoscopy) is hindered by lesions which mimic melanoma. Automatic discrimination of melanoma from mimics could allow detection of melanoma at an earlier stage. Seborrheic keratoses are common mimics; these have distinctive bright structures: starry milia-like cysts (MLCs). We report discrimination of MLCs from mimics by features extracted from starry MLC (star) candidates. After pre-processing, 2D template matching is optimized with respect to star template size, histogram pre-processing, and 2D statistics. The novel aspects of this research were new details for region of interest (ROI) analysis of the centers of the star candidate, a new method for determining shape of hazy objects and multiple template matching, using unprocessed ROIs, shape-limited ROIs, and histogram-equalized ROIs. Features retained in the final model for the decision MLC vs. mimic by logistic regression include star size, 2D first correlation coefficient, correlation coefficient to the star shape template, equalized correlation coefficient, relative star brightness, and statistical features at the star center. These methods allow optimization of MLC features found by 2D template correlation. This research confirms the importance of fine ROI features and ROI neighborhoods in medical imaging.

1 INTRODUCTION

Milia-Like Cysts (MLCs) are small white-to-ivory dermoscopic structures that are commonly seen in seborrheic keratoses (SKs). Their presence in benign lesions makes MLCs an attractive target to distinguish melanomas from benign lesions (Braun et al., 2002); (Menzies et al., 2008); (Stricklin et al., 2011). MLCs are classified as either starry or cloudy (Figure 1). Starry MLCs are < 1/3 mm in diameter, round and often appear like “stars on a misty night” (Stricklin et al., 2011). Stricklin et al. found that starry MLCs had 90.5% sensitivity and 45.7% specificity for seborrheic keratosis (Stricklin et al., 2011).

Analysis for automatic detection of these structures has not been reported. The most critical factor to aid detection is the brightness of these structures (Figure 1), followed in importance by size and shape.

2 IMAGES, PREPROCESSING

2.1 Data Sets and Images used

Sixty-six seborrheic keratoses and 34 melanomas acquired in the course of the study NIH CA153927-02A2 had MLC or MLC-mimicking structures. Contact, non-polarized dermoscopy images (3Gen, Dana Point CA) with 1024x768 resolution were used.

2.2 Lesion Processing, Noise Removal

As starry MLCs are white or yellow, the blue plane is chosen for maximum contrast (Lee, 2001). The lesion border contours and hair masks were manually drawn as in Stoecker et al. (2005). Bubbles were automatically detected by high intensity and sharp gradient; hairs were removed manually.

Subramanian V., H. Moss R., K. Rader R., K. Mahajan S. and V. Stoecker W..
Template Matching for Detection of Starry Milia-Like Cysts in Dermoscopic Images.
DOI: 10.5220/0004227504440448
In *Proceedings of the International Conference on Computer Vision Theory and Applications* (VISAPP-2013), pages 444-448
ISBN: 978-989-8565-47-1

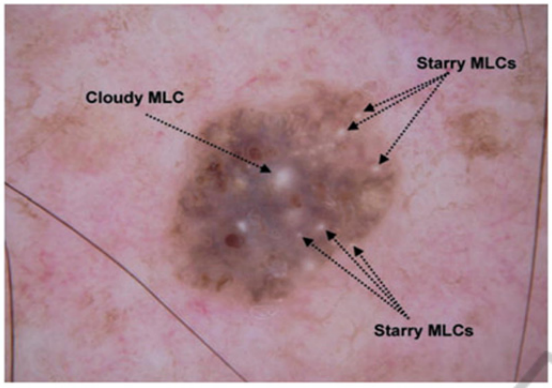

Figure 1: Seborrheic keratosis with a cloudy MLC and multiple starry MLCs (Stricklin et al., 2011).

3 CANDIDATE STAR SELECTION

3.1 Block-by-Block Selection of Candidate Pixels

The lesion area is divided into 13 × 13 pixel blocks; block size was empirically determined—as large as possible for computational efficiency, with upper bound constrained by the need to minimize MLC loss due to multiple MLCs within a block. The brightest pixel in each block is chosen as the center for a candidate starry MLC (star).

3.2 Lesion Area Mean Intensity as Threshold

Since stars are brighter than their surroundings, the number of candidate stars can be additionally reduced using a mean threshold, optimized at 0.85 × (lesion mean intensity). To avoid "salt and pepper" noise, a 3x3 mean filter was applied to the 3x3 neighborhood for each candidate pixel.

3.3 Rejecting Duplicate Candidates

If two candidate pixels occur in the same 13 × 13 block, the pixel with the highest intensity is designated as the candidate pixel and all other pixels are discarded.

4 STARRY MLC CHARACTERISTICS

To get more details about the star, the difference in intensity between consecutive concentric rings around the central pixel was calculated (Figure 2).

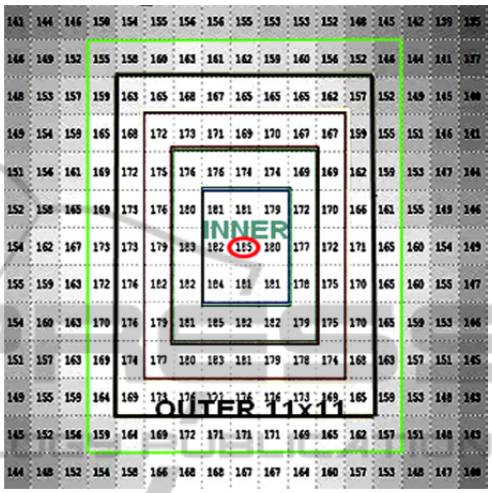

Figure 2: MLC concentric rings, 11x11 region lime-green, central pixel circled in red.

5 TEMPLATE MATCHING

The row vector method aided in star identification. To remove numerous false positive star mimics, the candidate stars were correlated with a star template.

5.1 Correlation Coefficient and its Significance

Correlation has been used extensively for template matching. Let f(x,y) be an image. Let w(x,y) be an object of interest. If object w is present in f, the correlation will be maximized at the location where w finds a correspondence in f. Matching is performed using the correlation coefficient $\gamma(x,y)$:

$$\gamma(x,y)\frac{\sum_s\sum_t[f(s,t)-\bar{f}(s,t)]\,[w(x+s,y+t)-\bar{w}]}{\{\sum_s\sum_t[f(s,t)-\bar{f}(s,t)]^2\ \sum_s\sum_t[w(x+s,y+t)-\bar{w}]^2\}^{1/2}}$$

where x = 0, 1, 2, 3 . . ., M-1, y = 0, 1, 2 . . ., N-1, M×N is the size of f, $\bar{w}$ is the mean value of pixels in w and $\bar{f}$ is the mean value of the region that is coincident with the current location of w. All summations are taken over the coordinates common to both f and w. The calculated correlation coefficient γ(x,y) is scaled such that the maximum

value is 1 and the minimum value is -1. $\gamma(x,y)$ is independent of amplitude in *f* and *w* (Gonzalez and Woods, 2002). Since amplitudes are normalized, $\gamma(x,y)$ depends only upon the match between shape and relative shading, as in Figure 2. If the candidate star has a similar shape and shading to the star template, the correlation coefficient will be close to 1. For starry MLCs, $0.7 < \gamma(x,y) \leq 1$.

5.2 Correlation with Different Star Templates

Since starry MLCs vary in size, each candidate star was correlated with star templates of sizes: 11×11, 17×17, and 23×23. The template with the highest correlation coefficient for that star was selected and the choice saved as 'star size.' Templates synthesized various ways, including actual MLC templates with and without rotation averaging and contrast enhancement, showed no difference in MLC screening results. Statistics on the central 11x11 star region were retained (Table 1).

5.3 Application of Range as a Threshold

All starry MLCs have a bright pixel at the center and radially decreasing intensity. The difference between maximum and minimum intensity, on the 0-1 intensity scale, for the 11×11 center of the star was determined. From 66 SK images, the data regarding the relative variation in pixel intensities in star centers were calculated. To be considered for further processing, a star must have a difference between the maximum and minimum pixel intensity values in the 11×11 star center exceeding 0.14, 0.075 and 0.03, for star sizes 11, 17 and 23, respectively. To illustrate the power of the central range threshold in star elimination, a SK after the first correlation had 34 candidate stars, whereas after applying the range threshold for the 11×11 star center, only 10 candidate stars remained, with no true stars eliminated. For 100 training images, fewer than 5% of the true starry MLCs were rejected.

6 CANDIDATE STAR SHAPE ANALYSIS

6.1 Shape of the Starry MLC

Star outlines are somewhat hazy (Figure 2). The drop in the intensity values with a radial outwards progression was not constant for all directions and was not constant among starry MLCs. Therefore, smoothing with a 3x3 mean filter applied with a sliding window and histogram equalization were performed, and the star shape was all points within 10% of the average intensity of the smoothed, equalized object (Figure 3). Features analyzed included area, perimeter, roundness ($Perimeter^2/4\pi$area), solidity, major and minor axis lengths, eccentricity, and major axis/equivalent diameter.

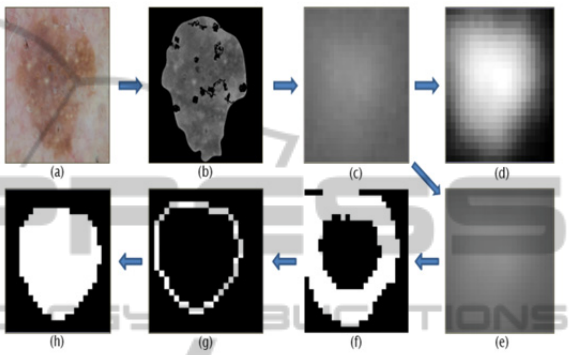

Figure 3: Formation of shape of the star for a true starry MLC. (a) Original image – Seborrheic Keratosis. (b) Lesion and bubble masks applied on blue plane. (c) Enlarged version of a starry MLC. (d) Histogram equalized starry MLC. (e) Enlarged version of smoothed starry MLC. (f) Initial shape of the star. (g) Thinned – one pixel width shape of the star. (h) Final filled centered star.

6.2 Second Correlation with Shape of the Star

Once the shape is determined, an ideal elliptical or circular binary star template is created, matching shape and orientation. If the difference between the major and minor elliptical axis is less than two pixels, the shape is considered circular. The original star candidate is correlated with this ideal star template. This second correlation yields two significant outputs: 1) Scaled output, to normalize the effect of different candidate star sizes, with scaling factors respectively 6, 4, and 3 for 11x11, 17x17, and 23x23 star candidates and 2) the candidate star is histogram-equalized to better differentiate skin pores from starry MLCs.

7 LOGISTIC REGRESSION ANALYSIS

Thirty-three parameters obtained by the preceding

analysis were analyzed by the Statistical Analysis System (SAS Institute, Cary, NC). The total number of candidate pixels analyzed by logistic regression was 1005 candidates from the seborrheic keratosis images and 473 candidates from the melanoma images. Significant features determined by logistic regression (Table I) and the corresponding receiver operating characteristic curve (Figure 4) are displayed. The area under the ROC curve for MLC vs. mimic discrimination is 88.2%.

Table 1: Significant features of logistic regression model.

Parameter	Chi-Square	Pr > Chi-Sq
Star size	24.6856	< .0001
First correlation coefficient with ideal star template	29.1704	< .0001
Intensity difference between star and surround	25.5965	< .0001
Mean of 11x11 star center	8.6837	0.0032
Variance of 11x11 star center	10.0570	0.0015
Rise time of 11x11 star center	30.8251	< .0001
Correlation coefficient to the star shape template	11.1896	< .0008
Equalized correlation coefficient	29.2425	< .0001

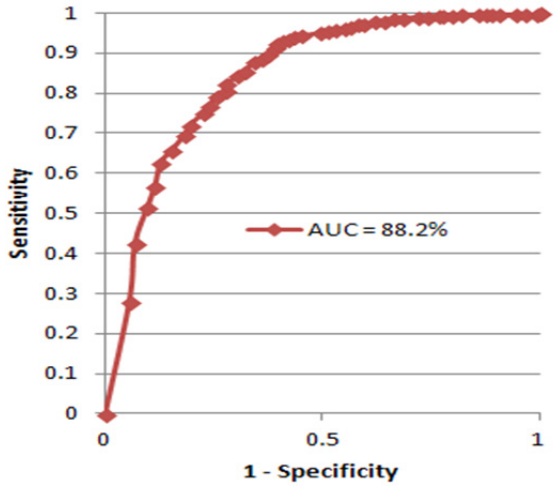

Figure 4: Receiver operating characteristic (ROC) curve for detection of starry MLCs vs. mimics.

8 CONCLUSION AND FUTURE WORK

This research was conducted to correctly classify benign SKs based on automatically detected starry MLCs. Well-known image processing techniques were employed. Yet these techniques were employed in novel ways: 1) new details for region of interest (ROI) analysis of the centers of star candidates, 2) template matching for size determination, 3) a new method for determining shape of hazy objects, and 4) performance of multiple template correlations using unprocessed ROIs, shape-limited ROIs, and histogram-equalized ROIs. Other methods such as subtraction of a filtered image from the original image were attempted, i.e. the LaPlacian of Gaussian method as a "tuning" filter for the fineness of detection. However, the differences between star ROIs and mimics are so tiny that fine details such as central star range are needed. Because of the fine discriminations needed, no simple filter or set of simple blob feature suffices to discriminate starry MLCs, and subtle intra-blob features were required.

The accuracy and the area under the receiver operating characteristic curve show that the algorithm presented here can identify most starry MLCs and allow accurate classification. Future work could increase MLC detection accuracy and benign vs. melanoma discrimination by investigating the following: 1) using a larger number of images, 2) using finer gradation of MLC sizes, 3) finding features of MLC mimics, e.g.. scales, 4) improving bubble masks, and 5) using additional color planes.

REFERENCES

Braun, R. P., Rabinovitz, H. S., Krischer, J., Kreusch, J., Oliviero, M, Naldi, L., … Saurat, J.H. (2002). Dermoscopy of Pigmented Seborrheic Keratosis: A Morphological Study. *Archives of Dermatology*, 138, 1556-1560.

Cheng, Y., Swamisai, R., Umbaugh, S. E., Moss, R. H., Stoecker, W.V., Teegala, S., Srinivasan, S.K. (2008). Skin lesion classification using relative color features. *Skin Research and Technology*, 14(1), 53-64.

Gonzalez, R. C. & Woods, R. E. (2002). *Digital Image Processing*. 2nd ed. New Jersey: Prentice Hall, pp. 698-704.

Lee, T. K. (2001). Measuring border irregularity and shape of cutaneous melanocytic lesions. Ph.D. Thesis, Simon Fraser University,Vancouver, British Columbia.

MATLAB version 7.8.0 (R2009a). 2009. Image Processing Toolbox. Natick, Massachusetts: The MathWorks Inc.

Menzies, S. W., Kreusch, J., Byth, K., Pizzichetta, M. A., Marghoob, A., Braun, R., …Johr, R. (2008). Dermoscopic evaluation of amelanotic and hypomelanotic melanoma. *Archives of Dermatology*, 144(9), 1120-7.

Stoecker, W. V., Gupta, K., Stanley, R. J., Moss, R. H., &Shrestha, B. (2005). Detection of asymmetric blotches (asymmetric structureless areas) in dermoscopy images of malignant melanoma using relative color. *Skin Research and Technology*, 11(3), 179-84.

Stricklin, S. M., Stoecker, W. V., Oliviero, M. C., Rabinovitz, H.S., & Mahajan, S.K. (2011). Cloudy and starry milia-like cysts: how well do they distinguish seborrheic keratoses from malignant melanoma? *Journal of the European Academy of Dermatology and Venereology*, 25(10), 1222-4.